HHS Public Access

Author manuscript

IEEE Trans Neural Syst Rehabil Eng. Author manuscript; available in PMC 2018 February 22.

Published in final edited form as:

IEEE Trans Neural Syst Rehabil Eng. 2014 July ; 22(4): 870–878. doi:10.1109/TNSRE.2014.2307256.

Estimation of Human Ankle Impedance During the Stance Phase of Walking

Elliott J. Rouse,
Member, IEEE

Levi J. Hargrove,
Member, IEEE

Eric J. Perreault, and
Member, IEEE

Todd A. Kuiken
Senior Member, IEEE

Abstract

Human joint impedance is the dynamic relationship between the differential change in the position of a perturbed joint and the corresponding response torque; it is a fundamental property that governs how humans interact with their environments. It is critical to characterize ankle impedance during the stance phase of walking to elucidate how ankle impedance is regulated during locomotion, as well as provide the foundation for future development of natural, biomimetic powered prostheses and their control systems. In this study, ankle impedance was estimated using a model consisting of stiffness, damping and inertia. Ankle torque was well described by the model, accounting for 98 ± 1.2% of the variance. When averaged across subjects, the stiffness component of impedance was found to increase linearly from 1.5 Nm/rad/kg to 6.5 Nm/rad/kg between 20% and 70% of stance phase. The damping component was found to be statistically greater than zero only for the estimate at 70% of stance phase, with a value of 0.03 Nms/rad/kg. The slope of the ankle's torque-angle curve—known as the quasi-stiffness—was not statistically different from the ankle stiffness values, and showed remarkable similarity. Finally, using the estimated impedance, the specifications for a biomimetic powered ankle prosthesis were introduced that would accurately emulate human ankle impedance during locomotion.

Index Terms

Biological system modeling; Prosthetic limbs; Quasi-stiffness; Stiffness; System identification

I. INTRODUCTION

The current level of understanding of the ankle joint's dynamic mechanical properties, known as joint *impedance*, may hinder the development of biomimetic prostheses and control systems. The ankle is an essential component of human locomotion, as the muscles spanning this joint provide the majority of mechanical power [1], and are important for vertical support and forward propulsion of the body [2]. Previous research spanning many

decades has provided a rich knowledge of ankle joint kinematics and kinetics [3–6]. However, little is known regarding how ankle impedance is modulated during walking. The need to understand ankle impedance during walking is underscored by the recent development of powered ankle prostheses [7–10]. Determining the natural impedance of the human ankle during walking is needed to provide the biologically-inspired rationale for the control of these devices. Currently, the impedance of these devices is governed by sophisticated control systems that model muscle behavior [11], emulate user-specific spring and damper values [9], or use phase plane invariants [12]. Without knowledge of the ankle's impedance during walking, there is no comparison for ascertaining the biological realism of these controllers.

Estimation of joint impedance requires an external perturbation; the joint is disturbed by a position or torque disturbance and system identification analyses are used to estimate impedance. Linear techniques may represent impedance in terms of a transfer function, an impulse response function, or a parameterized mechanical system—typically consisting of inertial, damping, and stiffness values [13]. Previous studies have estimated ankle impedance in several static postures [14–16] and have investigated the sensitivity of impedance to many factors, including mean ankle position [17, 18], displacement amplitude [19], torque [20] and neural activation [21]. These studies have shown ankle impedance to be positively correlated with the neural activation of the muscles crossing the ankle [20, 21] and negatively correlated with perturbation amplitude [19]. Using time-varying techniques, MacNeil et al. [22] estimated the ankle's impulse response function while supine subjects rapidly changed ankle torque. This technique was also used to estimate time-varying ankle impedance during a large imposed movement [23], where the low frequency impedance gain was shown to increase by 60% throughout the displacement. These studies elucidate how ankle impedance changes with respect to non-stationary conditions, but it is unclear if these results, obtained with the subject in a supine position, are relevant to locomotion during which it is difficult to apply the external perturbations required to estimate impedance.

Rather than perturbing the ankle during locomotion, researchers have instead focused on the torque-angle relationship of this joint [24–27], which is easier to obtain. Based on this characteristic curve, the ankle has been modeled as a first-order system with a passive stiffness matched to the slope of the torque-angle relationship. This slope is often known as the *quasi-stiffness* [26, 28, 29]. Hansen et al. [26] previously showed how the ankle's torque-angle relationship varied with walking speed. Interestingly, the torque-angle relationship was approximately linear for the majority of stance phase at normal walking speeds. This work provided insight into how ankle torque and angle co-vary during locomotion and established a foundation for the development of passive ankle prostheses, but did not provide any information about the impedance of the ankle. Since human joints are actuated by muscles, they are active rather than passive, and the joint stiffness (i.e. static component of impedance) cannot be estimated by analysis of the torque-angle relationship without a perturbation [29]. Therefore, in the context of human joint dynamics, the stiffness and quasi-stiffness are distinct entities during conditions of dynamic muscle activation, such as locomotion.

The objective of the present study was to estimate the impedance of the human ankle during the stance phase of walking. The impedance was estimated at four points during stance phase and the values were compared. Our hypothesis was that the impedance parameters would vary throughout stance phase, as a result of the corresponding changes in muscle activation and ankle angle. The intent of this work was to provide the foundation for the design and control of natural, biomimetic powered prostheses, as well as provide a comparison of the ankle's stiffness and quasi-stiffness values.

II. METHODS

A. Experimental

1) Apparatus—Impedance was estimated using perturbations applied by a mechatronic platform, termed the Perturberator Robot, validated and previously described in [30] and briefly summarized here. The robot has a single degree of freedom that can apply a rotational perturbation to the ankle when a subject is in contact with a hinged platform. A portable force platform was fixed to the hinged platform and the angle of the hinge was driven by an AC gear-motor. The motor was controlled using a commercial servodrive (model: AKD-B00606, Kollmorgen, Radford, VA) that received position control instructions from a microcontroller (model: PIC32, Microchip Technology, Inc., Chandler, AZ). The Perturberator Robot was recessed into an aluminum walkway, such that the platform section of the robot was flush with the surface of the walkway (Fig. 1).

2) Protocol—Ten healthy, able-bodied subjects (five male, five female) ranging from 24 to 32 years old and with no history of neurological impairment or lower extremity injury took part in this study. Subjects gave written, informed consent to all procedures, and the experiment was approved by the Northwestern University Institutional Review Board. Each subject wore a safety harness fastened to an overhead gantry system that statically exerted less than two Newton's of force on the subject.

Subjects' right ankles were instrumented with an electrogoniometer (Delsys, Boston, MA) to record ankle angle. One end of the device was securely fastened to the shank, while the other end was secured to the side of the foot. The sensor was previously calibrated using a protractor as an independent angle measure (sensitivity: 1.05 rad/V, with 95% confidence interval: ±0.09 rad/V), and shown to have an angular precision of 2.6×10^{-3} radians for small displacements [30]. To prevent slippage on the platform, subjects wore treaded cloth hospital socks (Medichoice, Mechanicsville, VA). Subjects set a metronome to a self-selected pace of between 85 and 90 steps per minute and were instructed to attempt to match walking frequency to the metronome. Subjects walked across a walkway approximately 5.25 m in length that included the recessed Perturberator Robot (Fig. 1). The starting position for each subject was adjusted such that when the heel of the subject's foot struck the force platform, on average, the center of rotation of the subject's ankle aligned with the center of rotation of the Perturberator robot. The vertical height of the robot's center of rotation was fixed at approximately 90 mm. When subjects stepped on the force platform a 0.035 radian (2°) perturbation was randomly applied to the right foot with a probability of 50%; dorsiflexion and plantarflexion perturbations occurred with equal probability. The duration

of the ramp portion of the perturbation was 75 ms and the constant velocity portion of the ramp was approximately 0.8 rad/second. Four perturbation timing points in stance phase were investigated corresponding to 100, 225, 350, and 475 ms following heel strike. These points were chosen to provide insight throughout stance phase, while the foot was in contact with the ground (i.e. before substantial heel rise). For trials in which a perturbation occurred, the timing point was chosen randomly with each point having equal probability. One hundred perturbation trials were recorded at each timing point with approximately 50% in each direction. Subjects were encouraged to rest after every 40 perturbation trials. The data acquired included all force platform data, motor angle, ankle angle, all sampled at 1 kHz with a 16-bit data acquisition system (model: USB-6218, National Instruments, Austin, TX) run through MATLAB (The Mathworks, Natick, MA). Lastly, high-definition video was recorded of foot placement on the Perturberator robot.

B. Analytical

All data were low-pass filtered using a bi-directional fourth order Butterworth filter with a cutoff frequency of 20 Hz and were segmented to include a 100 ms window beginning with the ramp perturbation. Forces caused by the intrinsic impedance of the robot were removed using linear filters estimated from data obtained when no subject was present [30, 31]. Ankle torque was determined by resolving the ground reaction force to the equivalent force-torque at the ankle's center of rotation;

$$T = F_z \delta_x + F_x \delta_z \quad (1)$$

where T is the torque about the ankle, F_Z and F_X are the z-axis (vertical) and x-axis (anterior-posterior direction) components of the ground reaction force, respectively; and δ_Z and δ_X are the distances in the z-axis and x-axis dimensions, respectively, from the center of pressure to the center of rotation of the ankle (Fig. 2). Plantarflexion is in the negative angular direction and angle was zeroed upon heel strike. Ankle torques determined in this manner have been shown to have negligible differences compared to inverse dynamics analysis [32]. The center of pressure (COP) and force information were obtained using the force platform. The COP information in the x-axis was referenced to the foot's coordinate system by subtracting the distance from the location of heel strike to the center of rotation of the ankle. This was determined by measuring the distance from heel contact to the subject's ankle center of rotation in software using the high-definition video.

1) Estimation—The estimation of ankle impedance depended on the isolation of the perturbation angle and torque response. That is, the torque and angle profiles that occurred naturally as a result of walking needed to be removed (Fig. 3, black). This removal was accomplished by subtracting the average unperturbed torque and angle profiles from the average of perturbation trials. A bootstrapping technique was used to estimate variability. A random selection of the angle and torque profiles from 60% of the perturbed trials for a specific timing point and perturbation direction were selected and averaged together. From these averaged angle and torque profiles, the average non-perturbed angle and torque profile was subtracted. The resultant angle and torque profiles had any offset removed such that

both began with zero. This technique was repeated 100 times for each timing point, each iteration differing in the specific perturbation trials included in the averaging. The resultant profiles were then used to obtain estimates of impedance. These methods were previously validated and shown to accurately estimate the stiffness of a prosthetic foot at several points during the stance phase of walking with an average error of 5% [30].

Following the isolation of the torque and angle perturbation response, a second order parametric model was assumed to characterize the impedance of the ankle

$$T_p = I_{tot}\ddot{\theta}_p + b_a\dot{\theta}_p + k_a\theta_p, \quad (2)$$

where T_p is the torque response to the perturbation, I_{tot} is the total inertia of the foot and other coupled body segments; and b_a and k_a are the damping and stiffness coefficients of impedance, respectively; finally, θ_p is the angular perturbation displacement of the ankle. A second-order model was chosen because it has historically been shown to provide high quality estimates of ankle impedance during postural studies [13, 19, 33, 34]. The derivatives were computed numerically in MATLAB by fitting a second order polynomial to four points surrounding each time point, and the polynomial coefficient was used to quantify the derivative [35]. The impedance parameters were estimated using least squares estimation over the 100 ms window [36]. Variance accounted for (VAF) was used to quantify the agreement of the model with the experimental results.

Finally, quasi-stiffness values for each subject were determined by taking the slope of the non-perturbed torque-angle relationship, $dT_w/d\theta_w$, where T_w is the torque about the ankle during walking and θ_w is the angle of the ankle during walking at each timing point (Fig. 4). The torque-angle relationship was obtained by averaging 60% of the non-perturbed trials, similar to the bootstrapping procedure mentioned above.

2) Statistics and Comparisons—Our primary objective was to quantify changes in ankle impedance throughout stance phase. Statistically, this was accomplished using a general linear model to evaluate stiffness, damping and inertia at each of the measured time points during stance. For this analysis, the time point and the perturbation type (dorsiflexion, plantarflexion, no perturbation) were treated as fixed factors, and subject as a random factor with the model including the interaction between time point and perturbation type. Each of the three impedance parameters were considered as a dependent variable; separate analyses were completed for each parameter. Bonferronni corrections were used for post-hoc comparisons, and the significance level for all tests was set at 0.05.

A sensitivity analysis of the filter parameters used in the identification procedure was completed to assess the effect on estimates. The identification procedure was re-computed for each of the following conditions: a 20% change in the filter cutoff frequency (20 Hz to 24 Hz), a 25% change in the filter order (fourth order to third).

For convenience, impedance values are presented as a function of stance phase percentage, rather than time since heel strike. Stance phase percentage was determined by averaging

stride duration across subjects. The mean stance duration was approximately 750 ms with a standard deviation of 24 ms.

III. RESULTS

The ankle impedance was well characterized by the second order model consisting of stiffness, damping and inertia. Representative angle and torque response profiles are shown in Fig. 5. The sine-wave like component of the torque response is a result of the perturbation's angular acceleration profile (i.e. inertial torque). When averaged across subjects and timing points, the variance accounted for (VAF) was 98±1.2%, demonstrating the quality of the model fit.

The stiffness component of impedance increased linearly throughout the region of stance phase tested (Fig. 6A). Bodyweight-normalized stiffness estimates were consistent across subjects, as indicated by the small standard deviations in Fig. 6A, especially for the earlier portions of stance. Stiffness increased by a factor of four from 20% to 70% of stance phase, starting at approximately 1.5 Nm/rad/kg and increasing to 6.5 Nm/rad/kg. When averaged across subjects, timing points and perturbation directions, the mean intra-subject variation (standard-deviation) of stiffness estimates was found to be 0.60 ± 0.45 Nm/rad/kg. Across subjects, stiffness varied significantly with respect to timing point ($p < 0.001$, $F_{3,116} = 22.7$), but not perturbation type ($p = 0.65$, $F_{2,117} = 0.43$). There was also no significant interaction between timing points and perturbation types ($p = 0.42$, $F_{6,113} = 1.0$). Posthoc comparisons of the differences in timing points showed that the fourth timing point (70% of stance phase) was statistically different than the first and second timing points (20% and 37% of stance phase, all $p < 0.05$); there were no significant differences for the second and third timing points.

Similar to the stiffness estimates, the bodyweight-normalized quasi-stiffness values increased throughout stance phase (Fig. 6A). There was large inter-subject variability of the quasi-stiffness at 70% of stance phase. This variance is likely a result of the stance phase timing approaching the point at which the ankle's torque-angle curve reverses direction. In other words, the quasi-stiffness has a vertical asymptote just before the powered plantarflexion (i.e. "push off") region of stance phase and quasi-stiffness values determined during this region are susceptible to large magnitudes.

The mean damping estimates also increased during stance phase; however, the inter-subject averaged estimates from 20% to 54% of stance phase were not statistically different than zero. The estimates were not consistent across subjects denoted by the large inter-subject variability. When averaged across subjects, timing points and perturbation directions, the mean intra-subject variation of damping estimates was found to be 0.005 ± 0.003 Nms/rad/kg. Across subjects, damping varied significantly with respect to timing point ($p < 0.001$, $F_{3,76} = 11.7$), but not perturbation type (dorsiflexion or plantarflexion, $p = 0.13$, $F_{1,78} = 2.4$). There was also no significant interaction between timing points and perturbation types ($p = 0.57$, $F_{3,76} = 0.67$). Posthoc comparisons of the difference in timing points showed that damping at 70% of stance phase was different than all earlier timing points (all

$p < 0.01$); furthermore, the estimate at 70% of stance phase was different than zero, and was approximately 0.03 Nms/rad/kg (Fig. 6B).

mean inertia estimates remained relatively constant across perturbation timing points and directions (Fig. 6C), with consistent inter-subject variability. When averaged across subjects, timing points and perturbation directions, the mean intra-subject variation of inertia estimates was found to be 0.009 ± 0.004 kgm^2. Across subjects, inertia values showed a slight positive trend as stance phase progressed. However, the general linear model showed that inertia did not vary significantly across timing points ($p = 0.12$, $F_{3,76} = 2.0$), perturbation directions ($p = 0.50$, $F_{1,78} = 0.44$) or the interaction between timing points or perturbation directions ($p = 0.74$, $F_{3,76} = 0.42$).

Modification of the filter parameters had a moderate effect on estimated joint impedance values. When the filter cutoff frequency was increased by 20% and averaged across subjects, perturbation directions and timing points, the mean discrepancy was 6.2 ± 6.1%, 9.7 ± 8.6% and 5.8 ± 3.0% for stiffness, damping and inertia, respectively. When the filter order was increased by 25%, the mean difference averaged across all conditions and subjects was 3.1 ± 2.2%, 8.3 ± 7.2% and 1.4 ± 1.8% for stiffness, damping and inertia, respectively. For comparison, when the original analysis was re-computed, only differing in the random bootstrapping trial selections, the mean difference averaged across all conditions and subjects was 0.8 ± 0.3%, 1.1 ± 1.0% and 0.0 ± 0.0, for the respective impedance parameters.

Finally, to provide a reference approximation of how much each component of impedance contributed to the perturbation torque response, an analysis was completed. The stiffness component of impedance was responsible for the majority of the torque during the perturbation. Using the peak position, velocity and acceleration perturbation magnitudes, multiplied by the mean stiffness, damping and inertia values, respectively, the potential peak torque contributions were quantified. The stiffness component of impedance contributed approximately 67% of torque magnitude, while damping contributed approximately 1% and inertia contributed approximately 32%.

IV. DISCUSSION

This study investigated how ankle impedance is modulated during the foot-flat region of stance phase. Previous literature has shown that joint impedance is affected by many factors that change throughout the gait cycle, including joint position and muscle activation. As such, we hypothesized that ankle impedance would vary significantly during stance. Ankle impedance was estimated using perturbations and found to change significantly during the region of stance phase tested. Unexpectedly, the stiffness component of impedance was found to match the slope of the ankle's torque-angle relationship during walking, having a value that changes in direct proportion to the change in ankle angle during stance phase. As such, the ankle stiffness during the evaluated portion of stance phase behaved as a quadratic spring. These results have important implications for the design and control of biomimetic robotic prostheses, since the measured behavior of the intact ankles presented in this study can be easily replicated by an artificial system.

A. Stiffness Estimates

The stiffness estimates from the early part of stance (20% – 40%) were lower than or comparable to previously reported stiffness estimates made during quiet standing. During quiet standing, ankle stiffness values between 2.0 – 2.7 Nm/rad/kg have been reported [14, 15], assuming a typical bodyweight of 70 kg. The estimates obtained during the latter part of stance (40% – 70%) were greater than previously reported for quiet standing, but were still less than would be expected during active torque generation under isometric conditions. Weiss et al. [18] demonstrated that ankle stiffness increases linearly with voluntary torque generation during isometric contractions. Using their results, we were able to estimate the ankle stiffness corresponding to the ankle torques generated during locomotion, but found these predictions to be in error. The stiffness estimated during locomotion was only approximately half of what would be predicted based on the isometric torque-stiffness curve for the human ankle. This finding agrees with previous work reported by Bennett et al. [37, 38], who demonstrated that elbow stiffness decreases during movement, relative to that measured during the maintenance of posture. The reason for the decreased stiffness during movement is not clear. Reduced muscle activity during the early portion of stance [39], or reduced neural feedback during movement [40] may be contributing factors.

B. Comparisons of Quasi-stiffness and Stiffness

Our results show that the ankle stiffness during the evaluated region of stance phase is regulated to behave as a nonlinear spring with a position-dependent stiffness that is approximately equal to the quasi-stiffness. This behavior can be observed by comparing the stiffness and quasi-stiffness results in Fig. 6A. The equivalence of the stiffness and quasi-stiffness during these measurements was not expected, since the muscles about the ankle are active during locomotion, and joint stiffness is known to change substantially with activation [41]. While the physiological mechanisms underlying this behavior are unclear, it has important implications for the design of prosthetic ankles made to replicate the mechanical properties of an intact ankle. A least during the region of stance phase evaluated in this study (20% – 70%), the stiffness of the human ankle can be approximated by a quadratic spring (see Implications for prosthesis design and control subsection). Beyond the tested region of stance, the intact ankle generates powered plantarflexion, a behavior that cannot be replicated by only a spring-like control system.

C. Damping Estimates

Damping estimates also increased during the stance phase, though the average values were not significantly different from zero except for the last measured time point (70% of stance). Some subjects even had negative values for damping estimates at 20% and 37% of stance phase. The large inter-subject variance and negative values could reflect poor estimates, as have commonly been reported in the literature [42], [15], or the negative values could represent the addition of small amounts of energy necessary to maintain locomotion. For example, passive dynamic walkers are able to “walk” with minimal energy added via ambulation down a slope [43, 44]; low-magnitude negative damping values could provide the energy needed for similar locomotion over level ground. However, future studies

providing more accurate estimates of damping will be required before these possibilities can be delineated.

D. Inertial Estimates

The investigation of ankle-foot inertia values was not a core objective of this study; however the inertia values remained consistent across subjects and timing points. Inertia values obtained were greater than the approximate inertia of the foot alone (~0.015 kgm^2, [45]); indicating that some of the inertia estimated may represent other coupled body segments or the mechatronic platform. Mean inertia values did not differ significantly across timing points or perturbation directions which supports quality of the estimates.

E. Implications for Prosthesis Design and Control

The spring-like stiffness values simplify the design and control of biomimetic powered ankle prostheses. Using linear regression to model the average data presented in Fig. 6A, the bodyweight-normalized stiffness as a function of ankle angle was determined to be

$$k_a = 13.6\theta_w + 1.6, \quad (3)$$

with an $R^2 = 0.98$; where k_a is the normalized stiffness of the ankle (Nm/rad/kg). This linear stiffness function denotes a quadratic spring relationship between angle and torque.

Equation (3) lays the foundation for the design and control of a biologically-inspired ankle prosthesis. For example, a series-elastic ankle prosthesis that included a series stiffness tuned to the biological ankle stiffness function could minimize the mechanical work required by an electric motor within a powered prosthesis [46, 47]. Additionally, a control system may be used to emulate this mechanical behavior. To this end, a biomimetic impedance controller was defined, where the impedance control equation governing the ankle torque would be

$$T_w = k_a(\theta_w - \theta_0) + b_a\dot{\theta}_w \quad (4)$$

θ_0 is the equilibrium position of the stiffness element. Using the non-perturbed ankle angle and torque information, the equilibrium angle was calculated by solving (4) for the equilibrium position. The equilibrium position was found to be approximately invariant from 20% – 70% of stance phase, with an average value of 0.075 ± 0.03 radians (this relative invariance follows as a result of the spring-like behavior of the ankle during stance phase). Neglecting the damping component of impedance, eqs. (3) and (4) were used to predict ankle torque during the investigated region of stance phase in the trials when no perturbation occurred (Fig. 7). The model-predicted torques were in agreement with the experimental data for most subjects. Thus, the stiffness function and impedance controller are parameterized by θ, promoting the development of a robust biomimetic design and control of powered ankle prostheses.

F. Limitations

The methods used in this study rely on several assumptions. Previous studies have shown that ankle impedance varies with many factors previously noted [17–21]. Furthermore, more recent studies have shown the non-linear and time-varying nature of ankle impedance [23, 48–51]. In the current study, we assume quasi-static, second-order dynamics despite changes to the conditions defining the joint's state (i.e. angle, torque, activation). The rationale behind this decision comes from the previous success of such techniques in estimating ankle impedance in static conditions [13], as well as practical limitations of applying the perturbations needed for more sophisticated analyses. Thus, the proposed methods provide a suitable first step in the ongoing investigation of ankle impedance during locomotion and future work will focus on implementing more sophisticated, time-varying [52] or nonlinear methods [49].

The filter parameters were chosen to preserve data content while filtering unwanted noise. The selection of filter parameters was based on previous validation studies that reported accuracy within 5% [30]. The impedance values reported in this study were moderately sensitive to the selection of these parameters, suggesting that they may contribute to error in the impedance estimates. The analysis was more sensitive to the cutoff frequency when compared to filter order, which is consistent with analyses where multiple derivatives are calculated.

At 70% of stance phase, there is greater inter-subject variability of impedance values, which may indicate error in the estimates. During terminal stance phase (50% – 80% of stance [53]), heel rise occurs and the foot flexes about the metatarsophalangeal and tarsometatarsal joints. This joint flexion may cause a discrepancy between the measured angle of the ankle and measured torque. Additionally, such variability may arise from an increase in the mechanical coupling with other segments (i.e. shank). Further studies are needed to understand how ankle impedance changes with joint flexion and variations in joint mechanical coupling.

When subjects stepped onto the force platform on the Perturberator Robot, the location of heel contact varied. The starting location of each subject was adjusted such that, on average, the center of rotation of their ankle aligned with the rotation axis of the robot. Slight variations in each trial caused some discrepancy between the center of rotation of the subjects' ankle and the rotation axis of the robot. The inter-subject average misalignment of rotation axes was 1.75 cm ± 1.56 cm. Previous studies quantifying the sensitivity of this misalignment using the Perturberator Robot have shown that ankle stiffness decreases by 6% per cm of misalignment during standing impedance estimation [31]. Therefore, this work predicts potential stiffness errors of 10.5% ± 9% as a result of misalignment.

The source of the ankle's impedance presented in this work cannot be completely determined; that is, there is no separation of the intrinsic and reflex components of impedance. We believe that the estimated ankle impedance is likely to be dominated by the intrinsic mechanics of the muscles and passive tissues crossing the ankle joint, rather than reflex contributions. The shortest latency reflexes occur at approximately 40 ms following an externally imposed movement [54, 55] and peak muscle force in the triceps surae muscles

occurs approximately 60 ms later [56, 57]. Since our analysis window was restricted to 100 ms following perturbation onset, any existing reflex contribution would have a limited impact on the measured torque considered in this study. During isometric conditions, reflexes have been shown to contribute 30 – 50% of the net torque measured at the ankle [58], but these pathways are known to be suppressed during movement [40] and when cocontraction is present [59, 60], conditions relevant to the stance phase of walking. These additional factors would likely further reduce the contributions of reflex mechanisms in the results reported in this manuscript, though we certainly do not discount their torque response contributions to ankle perturbations during unrestricted locomotion or other tasks for which reflex responses are known to be more substantial [58].

Acknowledgments

The authors wish to thank Dr. Jonathon Sensinger for his invaluable scientific and technical assistance.

VI. REFERENCES

1. Winter DA. Energy generation and absorption at the ankle and knee during fast, natural, and slow cadences. Clin Orthop. 1983; (175):147.
2. Neptune R, Zajac F, Kautz S. Muscle force redistributes segmental power for body progression during walking. Gait Posture. 2004; 19(2):194–205. [PubMed: 15013508]
3. Mann RA, Hagy J. Biomechanics of walking, running, and sprinting. The American journal of sports medicine. 1980; 8(5):345–350. [PubMed: 7416353]
4. Kadaba MP, Ramakrishnan H, Wootten M. Measurement of lower extremity kinematics during level walking. J Orthop Res. 1990; 8(3):383–392. [PubMed: 2324857]
5. Eng JJ, Winter DA. Kinetic analysis of the lower limbs during walking: what information can be gained from a three-dimensional model? J Biomech. 1995; 28(6):753–758. [PubMed: 7601875]
6. Murray MP, Drought AB, Kory RC. Walking patterns of normal men. The Journal of Bone and Joint Surgery (American). 1964; 46(2):335–360.
7. Au S, Herr H. On the design of a powered ankle-foot prosthesis. The Importance of series and parallel motor elasticity. IEEE Robotics and Automation Magazine. 2008; 15(3):52–59.
8. Au, SK., Weber, J., Herr, H. Biomechanical Design of a Powered Ankle-Foot Prosthesis. Proceedings of 2007 IEEE 10th International Conference on Rehabilitation Robotics; 2007. p. 298-303.
9. Sup F, Bohara A, Goldfarb M. Design and control of a powered transfemoral prosthesis. The International journal of robotics research. 2008; 27(2):263–273. [PubMed: 19898683]
10. Hitt JK, Sugar TG, Holgate M, Bellman R. An active foot-ankle prosthesis with biomechanical energy regeneration. Journal of Medical Devices. 2010; 4:011003.
11. Eilenberg MF, Geyer H, Herr H. Control of a Powered Ankle–Foot Prosthesis Based on a Neuromuscular Model. Neural Systems and Rehabilitation Engineering, IEEE Transactions on. 2010; 18(2):164–173.
12. Holgate MA, Sugar TG, Bohler A. A novel control algorithm for wearable robotics using phase plane invariants. 2009:3845–3850.
13. Kearney RE, Hunter IW. System identification of human joint dynamics. Crit Rev Biomed Eng. 1990; 18(1):55–87. [PubMed: 2204515]
14. Loram ID, Lakie M. Direct measurement of human ankle stiffness during quiet standing: the intrinsic mechanical stiffness is insufficient for stability. The Journal of Physiology. 2002; 545(3): 1041–1053. [PubMed: 12482906]
15. Casadio M, Morasso PG, Sanguineti V. Direct measurement of ankle stiffness during quiet standing: implications for control modelling and clinical application. Gait Posture. 2005; 21(4): 410–424. [PubMed: 15886131]

16. Roy A, Krebs HI, Bever CT, Forrester LW, Macko RF, Hogan N. Measurement of passive ankle stiffness in subjects with chronic hemiparesis using a novel ankle robot. J Neurophysiol. 2011; 105(5):2132–2149. [PubMed: 21346215]
17. Weiss PL, Kearney RE, Hunter IW. Position dependence of ankle joint dynamics--I. Passive mechanics. J Biomech. 1986; 19(9):727–735. [PubMed: 3793747]
18. Weiss PL, Kearney RE, Hunter IW. Position dependence of ankle joint dynamics--II. Active mechanics. J Biomech. 1986; 19(9):737–751. [PubMed: 3793748]
19. Kearney RE, Hunter IW. Dynamics of human ankle stiffness: variation with displacement amplitude. J Biomech. 1982; 15(10):753–756. [PubMed: 7153228]
20. Hunter IW, Kearney RE. Dynamics of human ankle stiffness: variation with mean ankle torque. J Biomech. 1982; 15(10):747–752. [PubMed: 7153227]
21. Weiss PL, Hunter IW, Kearney RE. Human ankle joint stiffness over the full range of muscle activation levels. J Biomech. 1988; 21(7):539–544. [PubMed: 3410857]
22. MacNeil JB, Kearney R, Hunter I. Identification of time-varying biological systems from ensemble data (joint dynamics application). Biomedical Engineering, IEEE Transactions on. 1992; 39(12): 1213–1225.
23. Kirsch RF, Kearney RE. Identification of time-varying stiffness dynamics of the human ankle joint during an imposed movement. Exp Brain Res. 1997; 114(1):71–85. [PubMed: 9125453]
24. Hobara H, Muraoka T, Omuro K, Gomi K, Sakamoto M, Inoue K, Kanosue K. Knee stiffness is a major determinant of leg stiffness during maximal hopping. J Biomech. 2009; 42(11):1768–1771. [PubMed: 19486983]
25. Gunther M, Blickhan R. Joint stiffness of the ankle and the knee in running. Journal of Biomechanics. 2002; 35(11):1459–1474. [PubMed: 12413965]
26. Hansen AH, Childress DS, Miff SC, Gard SA, Mesplay KP. The human ankle during walking: implications for design of biomimetic ankle prostheses. J Biomech. 2004; 37(10):1467–1474. [PubMed: 15336920]
27. Farley CT, Morgenroth DC. Leg stiffness primarily depends on ankle stiffness during human hopping. J Biomech. 1999; 32(3):267–273. [PubMed: 10093026]
28. Latash ML, Zatsiorsky VM. Joint stiffness: Myth or reality? Human Movement Science. 1993; 12:653–692.
29. Rouse EJ, Gregg RD, Hargrove LJ, Sensinger JW. The difference between stiffness and quasi-stiffness in the context of biomechanical modeling. IEEE Trans Biomed Eng. 2012; 60(2):562–568. [PubMed: 23212310]
30. Rouse EJ, Hargrove LJ, Perreault EJ, Peshkin MA, Kuiken TA. Development of a Mechatronic Platform and Validation of Methods for Estimating Ankle Stiffness during the Stance Phase of Walking. ASME Transactions on Biomechanical Engineering. 2013; 135(8)
31. Rouse EJ, Hargrove LJ, Akhtar A, Kuiken TA. Validation of methods for determining ankle stiffness during walking using the Perturberator robot. Proceedings of the IEEE International Conference on Biomedical Robotics and Biomechatronics. 2012:1650–1655.
32. Wells R. The projection of the ground reaction force as a predictor of internal joint moments. Bull Prosthet Res. 1981; 10:15. [PubMed: 7332827]
33. Agarwal G, Gottlieb C. Compliance of the human ankle joint. J Biomech Eng. 1977; 99:166.
34. Lee H, Ho P, Rastgaar M, Krebs HI, Hogan N. Multivariable Static Ankle Mechanical Impedance With Active Muscles. 2013
35. Scheid, F. Schaum's outline of theory and problems of numerical analysis. Vol. 1968. McGraw-Hill; 1968.
36. Ljung, L. System identification. Vol. 1999. Wiley Online Library; 1999.
37. Bennett DJ. Torques generated at the human elbow joint in response to constant position errors imposed during voluntary movements. Exp Brain Res. 1993; 95(3):488–498. [PubMed: 8224075]
38. Bennett D, Hollerbach J, Xu Y, Hunter I. Time-varying stiffness of human elbow joint during cyclic voluntary movement. Exp Brain Res. 1992; 88(2):433–442. [PubMed: 1577114]
39. Perry, J. Gait Analysis: Normal and Pathological Function. Vol. 1992. SLACK Incorporated; 1992.

40. Brooke JD, McIlroy WE, Collins DF, Misiaszek JE. Mechanisms within the human spinal cord suppress fast reflexes to control the movement of the legs. Brain Res. 1995; 679(2):255–260. [PubMed: 7633885]
41. Pfeifer S, Vallery H, Hardegger M, Riener R, Perreault EJ. Model-Based Estimation of Knee Stiffness. Biomedical Engineering, IEEE Transactions on. 2012; 59(9):2604–2612.
42. Krutky MA, Trumbower RD, Perreault EJ. Influence of environmental stability on the regulation of end-point impedance during the maintenance of arm posture. J Neurophysiol. 2013; 109(4):1045–1054. [PubMed: 23221409]
43. McGeer T. Passive Dynamic Walking. International Journal of Robotics Research. 1990; 9(2):62–82.
44. Collins S, Ruina A, Tedrake R, Wisse M. Efficient bipedal robots based on passive-dynamic walkers. Science. 2005; 307(5712):1082–1085. [PubMed: 15718465]
45. Winter, DA. Biomechanics and Motor Control of Human Movement. 2. Vol. 1990. John Wiley and Sons, Inc; 1990.
46. Rouse EJ, Mooney LM, Martinez-Villalpando EC, Herr HM. Clutchable Series-Elastic Actuator: Design of a Robotic Knee Prosthesis for Minimum Energy Consumption. Proceedings of the International Conference on Rehabilitation Robotics. 2013 In press.
47. Pratt, GA., Williamson, MM. Series elastic actuators. Intelligent Robots and Systems 95.'Human Robot Interaction and Cooperative Robots', Proceedings. 1995 IEEE/RSJ International Conference on; 1995; p. 399-406.
48. Hunter I, Korenberg M. The identification of nonlinear biological systems: Wiener and Hammerstein cascade models. Biol Cybern. 1986; 55(2):135–144. [PubMed: 3801534]
49. Westwick DT, Kearney RE. Nonparametric identification of nonlinear biomedical systems, part I: Theory. Crit Rev Biomed Eng. 1998; 26(3):153.
50. Baker, M., Zhao, Y., Ludvig, D., Wagner, R., Kearney, R. Book Time-varying parallel-cascade system identification of ankle stiffness from ensemble data. IEEE; 2004. Time-varying parallel-cascade system identification of ankle stiffness from ensemble data; p. 4688-4691.
51. Ikharia, BI., Westwick, DT. A bootstrap term selection method for the identification of time-varying nonlinear systems. Engineering in Medicine and Biology Society, 28th Annual International Conference of the IEEE; 2006. p. 3712-3715.
52. Ludvig, D., Perreault, EJ., Kearney, RE. Efficient estimation of time-varying intrinsic and reflex stiffness. Engineering in Medicine and Biology Society, EMBC, 2011 Annual International Conference of the IEEE; 2011. p. 4124-4127.
53. Perry, J. American Academy of Orthopaedic Surgeons. Atlas of Orthotics. 2. C.V. Mosby Company; 1985. Normal and pathological gait; p. 76-111.
54. Sinkjaer T, Andersen JB, Larsen B. Soleus stretch reflex modulation during gait in humans. J Neurophysiol. 1996; 76(2):1112–1120. [PubMed: 8871224]
55. Finley JM, Dhaher YY, Perreault EJ. Acceleration dependence and task-specific modulation of short-and medium-latency reflexes in the ankle extensors. Physiological Reports. 2013; 1(3)
56. Cavanagh P, Komi P. Electromechanical delay in human skeletal muscle under concentric and eccentric contractions. Eur J Appl Physiol. 1979; 42(3):159–163.
57. Kearney RE, Stein RB, Parameswaran L. Identification of intrinsic and reflex contributions to human ankle stiffness dynamics. IEEE Trans Biomed Eng. 1997; 44(6):493–504. [PubMed: 9151483]
58. Shemmell J, Krutky MA, Perreault EJ. Stretch sensitive reflexes as an adaptive mechanism for maintaining limb stability. Clin Neurophysiol. 2010; 121(10):1680–1689. [PubMed: 20434396]
59. Nielsen J, Sinkjær T, Toft E, Kagamihara Y. Segmental reflexes and ankle joint stiffness during co-contraction of antagonistic ankle muscles in man. Exp Brain Res. 1994; 102(2):350–358. [PubMed: 7705512]
60. Sinkjær T, Nielsen J, Toft E. Mechanical and electromyographic analysis of reciprocal inhibition at the human ankle joint. J Neurophysiol. 1995; 74(2):849–855. [PubMed: 7472388]

Biographies

Elliott J. Rouse (S′10 – M′12) received the B.S. degree in mechanical engineering from The Ohio State University, Columbus, OH in 2007, the M.S. degree in biomedical engineering from Northwestern University, Evanston, IL, in 2009 and the Ph.D. degree in biomedical engineering from Northwestern University in 2012, where he studied in the Center for Bionic Medicine. He is currently a Postdoctoral Associate in the Biomechatronics Group at the MIT Media Lab, Cambridge, MA. Dr. Rouse's primary research interests include the design and control of wearable robotic technologies, biomechanics, system identification and neural control of movement. His goal is to use joint impedance characteristics to inform the design and control of novel technologies to assist the disabled.

Levi J. Hargrove (S′05–M′08) received his B.Sc. and M.Sc. and PhD degrees in electrical engineering from the University of New Brunswick (UNB), Fredericton, NB, Canada, in 2003 2005, and 2007 respectively. He joined the Center for Bionic Medicine at the Rehabilitation Institute of Chicago in 2008. His research interests include pattern recognition, biological signal processing, and myoelectric control of powered prostheses. Dr. Hargrove is a member of the Association of Professional Engineers and Geoscientists of New Brunswick. He is also a Research Assistant Professor in the Department of Physical Medicine and Rehabilitation (PM&R) and Biomedical Engineering, Northwestern University. Evanston, IL, USA

Eric J. Perreault (S′97 – M′00) is Professor at Northwestern University, with appointments in the Department of Biomedical Engineering and the Department of Physical Medicine and Rehabilitation. He also is a member of the Sensory Motor Performance Program at the Rehabilitation Institute of Chicago.

Eric received his B.Eng and M. Eng degrees in Electrical Engineering from McGill University in 1989 and 1991, respectively. After working in industry for 4 years, he enrolled in the Biomedical Engineering Department at Case Western Reserve University, completing his PhD in 2000. From 2000–2002, he was a postdoctoral fellow in the Department of Physiology at Northwestern University. In 2010, he was a Visiting Professor at ETH Zürich.

Eric's current research focuses on understanding the neural and biomechanical factors involved in the control of multi-joint movement and posture and how these factors are modified following neuromotor pathologies such as stroke and spinal cord injury. The goal is to provide a scientific basis for understanding normal and pathological motor control that can be used to guide rehabilitative strategies and user interface development for restoring function to individuals with motor deficits. Applications include rehabilitation following stroke and tendon transfer surgeries, and user interfaces for neuroprosthetic control.

Currently, Eric is an Associate Editor for the IEEE Transactions on Neural Systems and Rehabilitation Engineering, and serves on the editorial boards for the Journal of Motor Behavior and the Journal of Motor Control. He also is a member of the IEEE Technical Committee on Rehabilitation Robotics.

Todd A. Kuiken received his MD and Ph.D. in biomedical engineering from Northwestern University (1990) and completed his residency in Physical Medicine and Rehabilitation at the Rehabilitation Institute of Chicago (1995). Dr. Kuiken currently is the Director of the Center for Bionic Medicine. He is a Professor in the Depts. of PM&R, Biomedical Engineering and Surgery of Northwestern University.

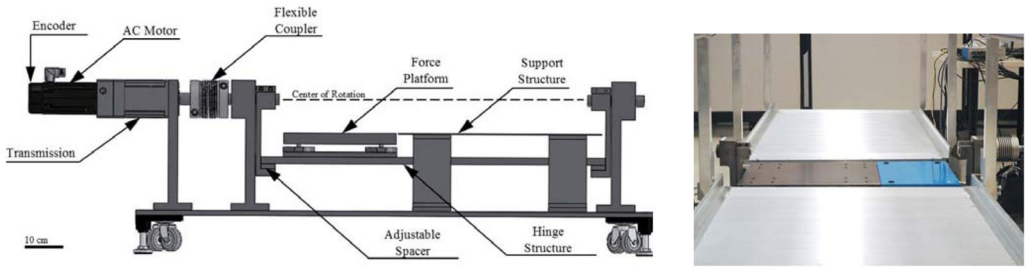

Fig. 1.

Left: Schematic of Perturberator Robot shown with relevant features highlighted, reprinted from [30]. Right: Perturberator Robot shown recessed into walkway. Total walkway length was approximately 5.25 meters.

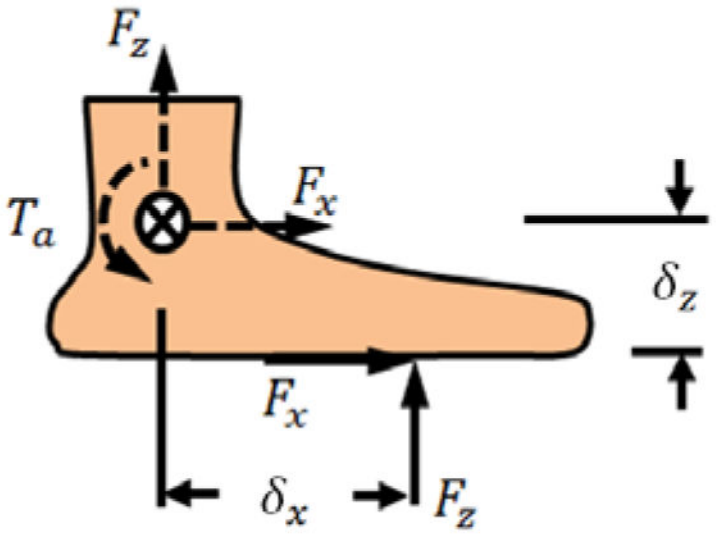

Fig. 2.

Diagram showing ground reaction forces acting on the foot (solid). The resultant (dashed) ankle torque, T_a, is computed by multiplying the ground reaction force components by their respective perpendicular distances.

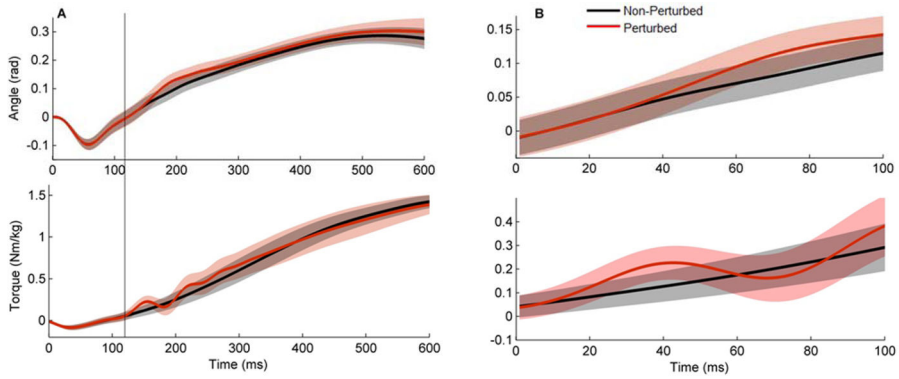

Fig. 3.

Mean values (bold) and standard deviations (translucent) for the non-perturbed trials (black line) and the first timing point with a dorsiflexion perturbation (red line) shown for a representative subject. Column A shows data from stance phase with perturbation onset denoted by the vertical line. Column B shows data during the analysis window. The impedance is estimated by the difference between the perturbed and non-perturbed data.

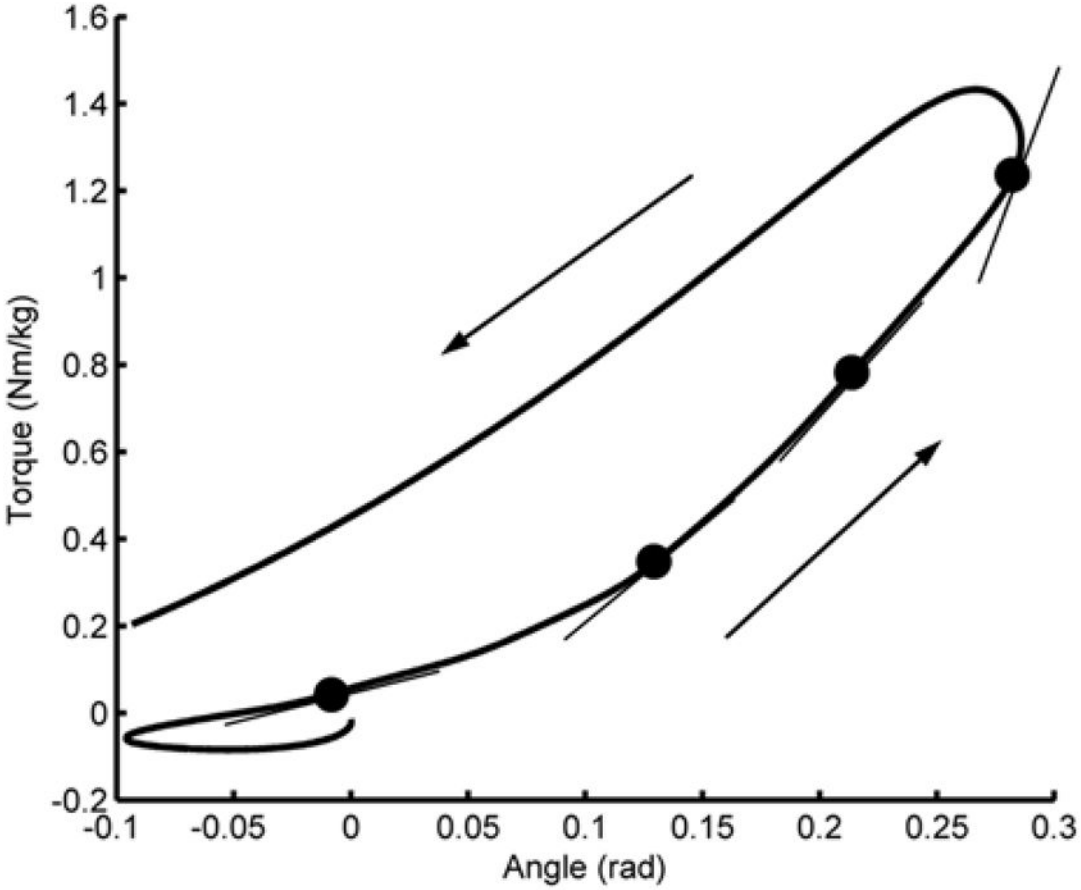

Fig. 4.

Average torque-angle relationship for a representative subject. The timing points are denoted by dots and the quasi-stiffness was calculated as the slope of the relationship at each timing point (thin black lines).

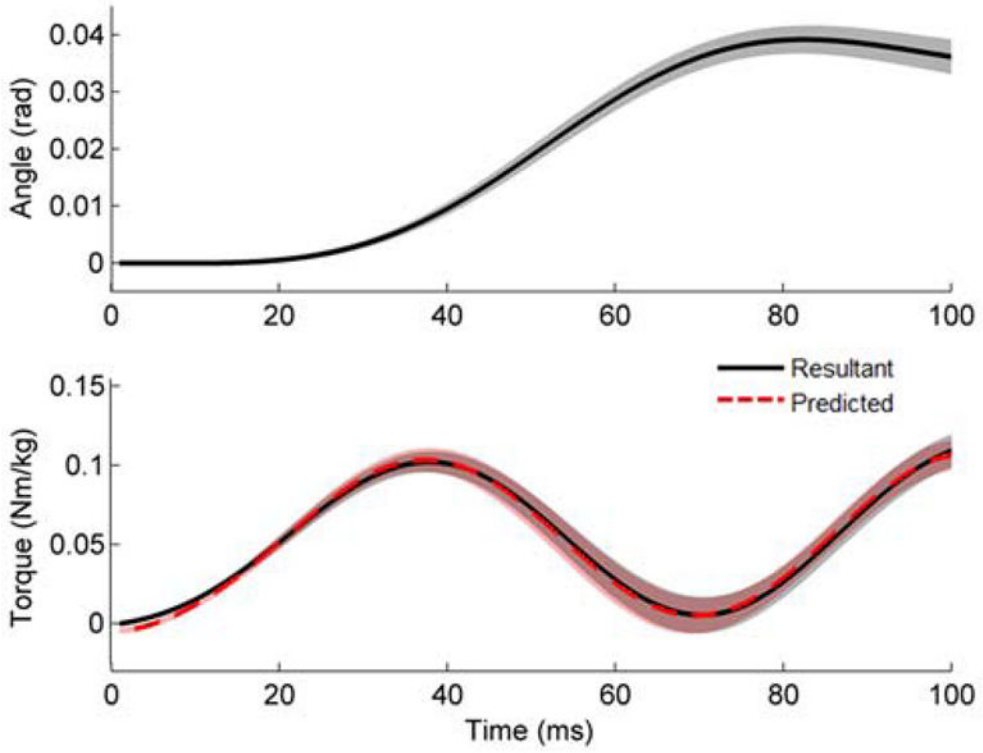

Fig. 5.

The resultant ankle angle (top) and resultant torque (bottom) plotted as a function of time for a representative subject and experimental conditions. The time window begins with the onset of the perturbation. The means are shown in bold with standard deviation in translucent. Note that these standard deviations reflect the variation in the mean of the bootstrap results, not the original data. The subject's resultant ankle angle and torque profiles are shown in black and the model predicted torque is shown in dashed red.

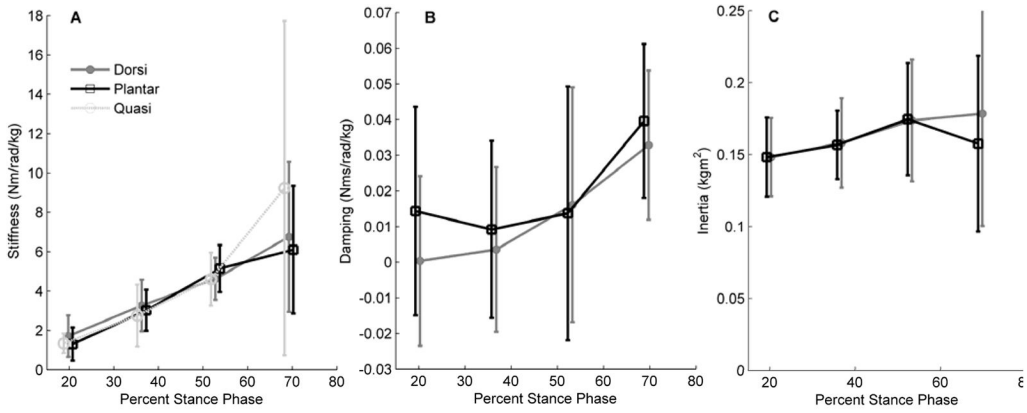

Fig. 6.

Inter-subject average stiffness (A), damping (B) and inertia (C) estimates as a function of percentage of stance phase. Error bars denote the standard deviation across subjects and are offset for clarity. Marker style denotes perturbation type, with ‘Quasi’ denoting values obtained without a perturbation (i.e. quasi-stiffness). Stiffness estimates increased linearly with stance phase and quasi-stiffness values and stiffness estimates were not different. Damping estimates increased, with only the estimates at 70% differing significantly from zero and inertia was not different across timing points or perturbation directions.

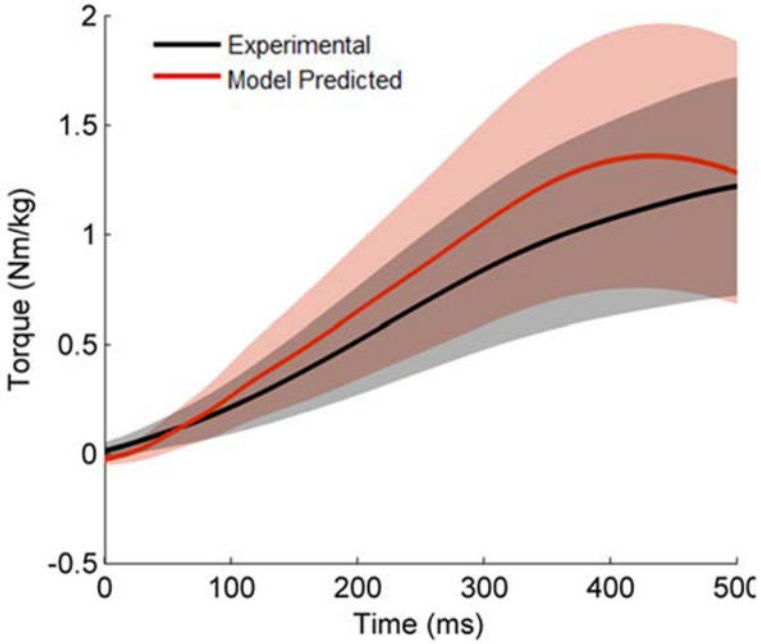

Fig. 7.

Model predicted experimental torques shown of a representative subject during the foot flat region of stance phase. The model predicted torques were generated using the impedance control equation and the quadratic spring relationship. Standard deviations are shown in translucent.